XIX ANIDIS Conference, Seismic Engineering in Italy

Experimental characterization of the mechanical behaviour of U-shaped dissipative devices

Nicola Buratti[a]*, Andrea Vittorio Pollini[b], Claudio Mazzotti[a]

[a]*DICAM, University of Bologna, Viale del Risorgimento 2, 40136 Bologna, Italy*
[b]*Sismo Solution s.r.l., Viale Angelo Masini 48, 40126, Bologna, Italy*

Abstract

Energy dissipation devices are used in earthquake engineering in order to reduce the negative effects of ground-motions on structures, thus limiting damage to structural and non-structural components. Different technologies have been proposed to this aim, i.e. viscous fluid dampers, friction-based dampers, hysteretic dampers, etc. Among the different solutions available the present paper focuses on a specific type of hysteretic dampers, U-shaped dissipators. They were first proposed in the 70s and to date have found limited application in the design practice, mainly in buildings with structural walls, exploiting the relative displacement between adjacent walls to dissipate energy.
The paper presents the results of an experimental campaign aimed at characterizing the mechanical behaviour of energy dissipators with linear movement, based on U-shaped steel plates. Different configurations were designed and tested, imposing displacement cycles of increasing amplitude. The paper discusses the observed energy dissipation capacity and the stability of the hysteretic cycles.

Keywords: Dissipative devices; energy dissipation; hysteretic cycles; experimental tests; U-shaped elements

1. Introduction

Seismic protection of structures using anti-seismic devices may allow to save lives and minimize damage to structures in case of earthquakes of high intensity. The possibility to reduce the effects of the seismic actions and to minimize damage to structural and non-structural elements through is particularly relevant in the seismic rehabilitation of existing industrial buildings where damage can determine also high economic impact due to business interruption.

Recent earthquakes have highlighted for example the high vulnerability of precast Reinforced Concrete (RC) structures not designed against seismic loads. Most of the partial- and full-collapses observed during past seismic events were caused by the absence of effective mechanical connectors between structural elements, in fact, friction-based connections were widespread (Bournas et al., 2013; Liberatore et al., 2013; Magliulo, Ercolino, et al., 2014; Savoia et al., 2017).

Given the high vulnerability of connections, many strengthening solutions have been proposed in the literature. Ligabue et al., 2014 proposed L-shaped steel elements for connecting beams to columns, Muciaccia et al., 2014 studied post-inserted metal anchors and fastenings, Bournas et al., 2013 introduced the use of cable restraints in order to reduce the possibility of loss-of-

---

* Corresponding author. Tel.: +39 051 2093248.
  E-mail address: nicola.buratti@unibo.it

support failures of roofing elements. Magliulo, Cimmino, et al., 2014 proposed beam-column mechanical connectors to avoid the loss of support failure of beams. Dal Lago et al., 2017 proposed to use steel angles as dissipative connection. Belleri et al., 2017 have proposed a recentering dissipative device based on rotary friction. Martinelli & Mulas, 2010 have proposed the insertion of devices that dissipate energy through rotary friction. Pollini et al.(2018 and 2021) proposed dissipative connectors based on carbon wrapped steel tubes. Mashal et al., 2019 proposed innovative metallic dissipaters for earthquake protection of structural and non-structural components based on UFPs encased by a hollow square or rectangle section sleeve, with the possibility to also incorporate self-centring.

The present paper presents connection devices that dissipate energy using U-shaped steel element. Their behaviour is first discussed from the theoretical point of view, then experimental tests are presented in order to describe their behaviour under cyclic actions and finally an application (patent pending industrial invention) as connectors for roofing elements is shown.

2. U-Shaped dissipative devices

2.1. Theoretical background

The U-shaped Flexural Plate (UFP) is a type of flexural dissipator proposed for the first time by Kelly (Kelly et al., 1972) as a mean of providing energy dissipation between structural concrete walls. Energy dissipation based on UFP found successful application in coupled rocking post-tensioned precast walls, in particular in the PREcast Seismic Structural Systems (PRESSS) (Priestley et al., 1999) and PRES-LAM (Palermo et al., 2005) research programs. The experimental program conducted for the PRESS program tested the behaviour of different connectors under a reverse cyclic vertical displacement history and the UFPs were found by (Schultz & Magana, 1994) to be one of the most suitable connectors, maintaining a stable cyclic force-displacement response up to large displacements while dissipating large amounts of energy.

UFPs are formed from bending a steel plate around a fixed radius to form a "U" shape. This is usually performed when the plates are hot to prevent stress concentrations in the final U shape. The element is initially in a semi-circular form with two equal straight sections on either side. When one side is subjected to a displacement relative to the opposite side, the semi-circular portion rolls along the plate and work is done at the two points where the radius of curvature is changed from straight to curved and vice versa. UFPs can be designed for a large range of possible displacements and forces by varying the plate thickness, width, and radius.

As highlighted by Baird et al. (2014) among the main reasons of the increasing use of UFPs for low-damage-design structures there are the production cheapness compared to other kind of energy dissipator devices, their large stable hysteretic behaviour, flexibility in application and replaceability.

In literature there are limited information available regarding the calculation of design values for U-shape elements, like initial and post-yield stiffness, capacity, and displacements. The force provided by a UFP was derived analytically by Kelly et al. (1972) by relating the coupling shear of the UFP to the plastic moment of the rectangular cross-section depending on the effective cyclic stress (σ), width (b), thickness (t), and average radius (R). The bending stress distribution for the plastic section capacity was assumed to be a rectangular stress block.

Therefore, the theoretical plastic moment of a UFP can be determined as:

$$M_p = \frac{\sigma_y b t^2}{4} \tag{1}$$

and the corresponding force

$$F_p = \frac{2M_p}{D} = \frac{\sigma_y b t^2}{4R} \tag{2}$$

For a rectangular section, the yield force is 2/3 the plastic force. Thus, the strength at first yield (F_y) can be calculated as:

$$F_y = \frac{\sigma_y b t^2}{6R} \tag{3}$$

The strength at first yield is important for calculating the theoretical initial stiffness of the element. The yield displacement and the initial stiffness of a UFP can be determined analytically using energy methods, in particular Castigliano's Second Theorem, as described by Baird et al. (2014)

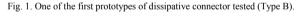$$\Delta_y = \frac{27\pi F_y (2R)^3}{16Ebt^3} \tag{4}$$

$$k_i = \frac{F_y}{D_y} = \frac{16Eb}{27\pi}\left(\frac{t}{2R}\right)^3 \tag{5}$$

As described by Kelly et al. (1972), the yield strength is not relevant when assessing the expected maximum strength of an element designed to have a cyclic behaviour since after a few loading cycles no defined yield point exists, but it is a very useful parameter during a preliminary design of the component. In fact, calculation of the initial stiffness is critical to ensure the device will activate at the expected displacements. The maximum force of a UFP device exceeds the yield and plastic force due to strain hardening of the steel. Tests performed by many researchers have shown that stresses are typically in the order of 145 – 215% that of the yield stress obtained from direct tension tests (Kelly et al., 1972; Pampanin et al., 2010). Accurately quantifying this maximum force is critical to identify capacity design principles.

Twigden and Henry (Twigden & Henry, 2015) proposed an estimate of the ultimate strength of a UFP can be derived from the plastic force equation by multiplying it by an overstrength factor which is equal to the ultimate stress (σ_u) divided by the yield stress.

$$F_u = F_p \frac{\sigma_u}{\sigma_y} \tag{6}$$

Experimental tests performed by Baird et al. (2014) showed that the plastic force predicted by Eq. 2 underestimates the maximum force in the UFP. Thus, they presented design equations based on a parametric study, to assist in the design of UFPs. This parametric study uses a combination of experimental testing and finite element analyses to verify analytically derived design formulae. The non-linear post-yield force-displacement behaviour of UFPs was found to be well represented by the Ramberg-Osgood function.

Fig. 1. One of the first prototypes of dissipative connector tested (Type B).

3. Experimental tests on the dissipative devices

In the first stage of the research UFP based dissipators with different shapes were tested. Fig. 1 shows an example of one of the first prototypes (Type B); it features two UFP steel dissipative elements with a thickness of 2 mm and a radius of 12 mm. These are supported by a steel fork and connected to a moving steel plate at the centre. Two steel plates are bolted to the two fork legs in to balance the horizontal forces produced by the UFP dissipative elements. Cyclic tests were carried out using an MTS Landmark servo hydraulic testing machine; in particular displacement cycles with amplitude 0.5 mm, 5 mm, 10 mm, 20 mm were imposed on the prototype, the first three cycles were repeated 5 times and the last cycle 10 times. The cycle with amplitude 0.5 mm was defined to maintain the dissipative elements elastic. Fig. 2 shows the force-displacement curves obtained from the tests, it can be noticed that they feature a relevant energy dissipation capacity and that cycles are in general stable with no relevant deterioration. It is also possible to observe that the behaviour is not fully symmetrical in terms of yielding force, which is about 8 kN in one direction and 7 kN in the opposite. For this reason, the geometry of the dissipative devices was modified, introducing a symmetrical layout of the UFPs and increasing the maximum displacement capacity. The so obtained prototype (Type A) featured four U-shaped elements with a thickness of 2 mm and a radius of 8 mm. Cyclic tests were carried out also on this device; the displacements imposed were 1 mm, 7.5 mm, 15 mm and 30 mm. Fig. 3 shows an example of the results obtained from one of the tests. Cycles are wide and stable also in this case, furthermore, comparing Fig. 2 with Fig. 3 it is possible to observe that, for the Type A prototype, the yielding force is symmetrical in the two directions. Further tests were carried out to evaluate the low-cycle fatigue capacity of the device, compared the minimum number of 10 cycles at the maximum displacement required for seismic dissipative devices; in this case 30 mm displacement cycles were imposed to the prototype until failure occurred. Fig. 4 shows an example of the results obtained, the device failed after 19 cycles at the maximum displacement, with the fracture of one of the U-shaped elements.
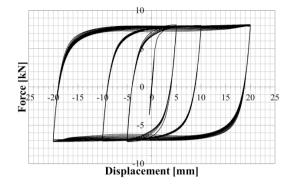
Fig. 2. Results of the cyclic experimental tests on the prototype Type B.
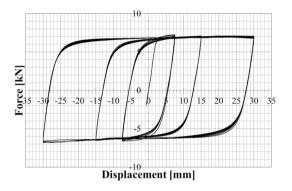

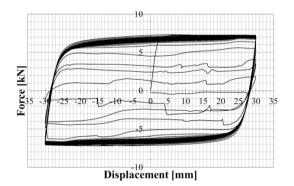Fig. 3. Results of the cyclic experimental tests on the prototype Type A.

Fig. 4. Results of the low-cycle fatigue tests on the prototype Type A.

Tab. 1. Comparison between experimental values and analytical values predicted by formulae.

UFP	R (mm)	t (mm)	F_y (kN)		F_p (kN)		Δ_y (mm)		k_y (kN/mm)	
			An.	Exp.	An.	Exp.	An.	Exp.	An.	Exp.
Type A	12	2	4.88	5.76	7.32	7.15	1.0	1.9	5.04	2.7
Type B	8	2	3.66	4.02	5.5	8	0.43	0.49	8.52	8.2

    Finally, Tab. 1 shows a comparison between the experimental results and the prediction of the analytical formulas discussed in Section 2. In general, only a limited agreement was observed. Generally, the analytical predicted force underestimates the experimental value. This, as described in previous section, is mainly due to the methodology used in identifying yielding point of the curve (not easy to be defined as the UFP presents a gradual change in stiffness) and to hardening in the steel cyclic response, that has a significant influence on predicted force and displacements values.

    To better predict the experimental behaviour of UFP dissipative elements, a FEM model was developed using ABAQUS (Fig. 5). A 3D deformable solid made up of 0.5 mm mesh elements was used to model the UFPs, while 2 mm and 5 mm mesh elements

were used for other elements (Fig.5, left panel). The geometry of the model was that of the UFP tested experimentally. A plastic isotropic yield model with cyclic hardening was used for all the steel elements and material properties were set based on the results of tensile tests. Contact interface elements were used to describe the interactions among the UFPs and the other elements. The numerical force-displacement curve of the UFP (Fig. 5, center panel) represents with good approximation the experimental results, capturing very well both the yielding and post-yielding. The best results were obtained increasing the yielding stress of the material to consider hardening, which occurs during the bending process. The Von Mises stresses at 20 mm displacement are depicted in the right panel of Fig. 5
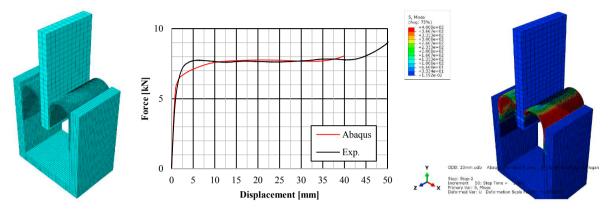

Fig. 5. FEM mesh (left), monotonic force-displacement curves (centre) and Von Mises stress distribution at 20 mm displacement (right) for the Type B device.

4. Experimental tests on a RC precast roofing element

The second part of the experimental campaign was focused on the characterization of the behaviour of the dissipative devices described in the previous sections, when used as dissipative connectors for reinforced concrete precast roofing elements. To this purpose we designed an experimental setup in which a simply supported portion of a π-shaped roofing element was tested under cyclic horizontal loads. The element was supported on two reinforced concrete elements and had two Type A devices at each end. Fig. 6 shows the experimental setup adopted while Fig. 7 illustrates a detail of the connection of one of the dissipative elements. Furthermore, it shows one of the LVDT displacement transducers used during the test to measure the relative horizontal displacement between the specimen and the supporting RC elements; 4 displacement transducers were used in total, two at each end of the specimen. Cyclic horizontal displacements were imposed to the specimens by means of a servo-hydraulic actuator that was connected to the specimen by means of two steel beams, one at each end, connected through prestressed steel bars. A load cell was installed on the servo-hydraulic actuator to measure the applied force. The specimen had a length of 4 m, corresponding to 50% of the length of an actual element, therefore an overload of 10 kN was applied (obtaining a total load of 30 kN) to produce vertical support reactions (i.e. 7.5 kN) consistent with those of an 8 m long roofing element.

Fig. 6. Experimental setup adopted for the tests on the precast RC roofing element equipped with UFP dissipative connectors: geometry of the roofing element (left) and steel beams used for attaching the specimen to the servo hydraulic actuator (right).

Fig. 7. Detail of the collection of one of the UFP dissipative devices to the precast RC roofing beam.

Two different support configurations were considered, i) concrete on concrete support, often found in Italy in precast RC structures non designed against seismic loads; ii) concrete on Teflon support, to reduce friction forces and better evaluate the behaviour of the dissipative devices. Before testing the roofing element equipped with the dissipative connection devices, preliminary tests were carried out to estimate the friction forces at the supports, in these tests three displacement cycles with amplitude 30 mm were imposed on the beam. Tests were in displacement control with a loading rate of 0.5 mm/s. Fig. 8 shows the force - displacement relationship obtained for the concrete-on-concrete test configuration. The friction threshold is about 19 kN (i.e. 4.75 kN per support), corresponding to a friction coefficient of about 0.6, and remains very regular during the tests. Fig. 9 shows the results of the concrete-on-Teflon tests, the friction threshold is in this case less regular during the cycles, with a maximum value of about 2 kN and a minimum value of 1 kN, corresponding to values of the friction coefficient values of 0.07 and 0.035, respectively. Since the highest values of the friction force were observed during the first loading and when cycles were reversed, we assume that the variation in the friction force may be due to the vertical deformability of the Teflon pads used, which might have produced a sort of mechanical interlock.
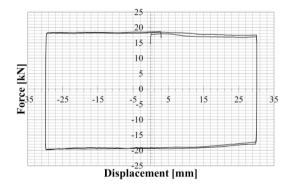

Fig. 8. Force displacement diagram for the test with no dissipative devices and concrete-on-concrete supports.
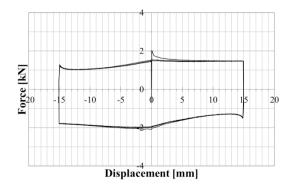

Fig. 9. Force displacement diagram for the test with no dissipative devices and concrete-on-Teflon supports.

The tests with the dissipative connectors were performed by imposing displacement cycles with increasing amplitude, i.e. 7.5 mm, 15 mm and 30 mm; each for the first two cycles was repeated 5 times and the last cycle 10 times. In general, the test on the roofing beam equipped with dissipative devices confirmed the behaviour observed during the tests discussed in Section 3. Fig. 10 shows the behaviour observed during the test with the concrete-on-concrete support; the effect of friction is clearly visible by comparing Fig. 10 with Fig. 8. Fig. 11 shows the results obtained from the Concrete-on-Teflon tests, where the contribution of friction is negligible compared to that of the connectors. In both cases no failure was observed during the tests.
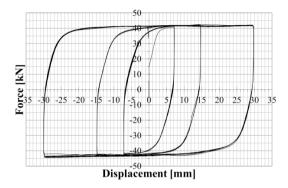

Fig. 10. Force displacement diagram for the test with dissipative devices and concrete-on-concrete supports.
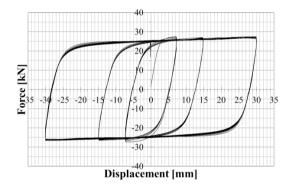

Fig. 11. Force displacement diagram for the test with dissipative devices and concrete-on-Teflon supports.

5. Conclusions

The present paper presented the results of experimental tests on dissipative connectors based on UFP dissipators, the tests showed that these devices have a stable hysteretic cycle with high energy dissipation capacity. Test results were compared with analytical predictions of the behaviour from the literature, but only limited agreement was found. The devices tested could be used as connectors for different types of structural and non-structural elements. As an example of their application the paper presented tests on a precast RC roofing element.

References

Baird, A., Smith, T. J., Palermo, A., & Pampanin, S. (2014). Experimental and numerical study of U-shape flexural plate (UFP) dissipators. *New Zealand Society for Earthquake Engineering Conference*.

Belleri, A., Marini, A., Riva, P., & Nascimbene, R. (2017). Dissipating and re-centring devices for portal-frame precast structures. *Engineering Structures*, *150*, 736–745. https://doi.org/10.1016/j.engstruct.2017.07.072

Bournas, D. A., Negro, P., & Taucer, F. F. (2013). Performance of industrial buildings during the Emilia earthquakes in Northern Italy and recommendations for their strengthening. *Bulletin of Earthquake Engineering*, *12*(5), 2383–2404. https://doi.org/10.1007/s10518-013-9466-z

Dal Lago, B., Toniolo, G., Felicetti, R., & Lamperti Tornaghi, M. (2017). End support connection of precast roof elements by bolted steel angles. *Structural Concrete*. https://doi.org/10.1002/suco.201600218

Kelly, J. M., Skinner, R. I., & Heine, A. J. (1972). Mechanisms of Energy Absorption in Special Devices for Use in Earthquake Resistant Structures. *Bulletin of the New Zealand Society for Earthquake Engineering*, *5*(3), 63–88.

Liberatore, L., Sorrentino, L., Liberatore, D., & Decanini, L. D. (2013). Failure of industrial structures induced by the Emilia (Italy) 2012 earthquakes. *Engineering Failure Analysis*, *34*, 629–647. https://doi.org/10.1016/j.engfailanal.2013.02.009

Ligabue, V., Bovo, M., & Savoia, M. (2014). Connessioni tegolo-trave: studio sperimentale e numerico del comportamento di angolari di collegamento (in Italian). *Proceedings of Workshop "Tecniche Innovative per Il Miglioramento Sismico Di Edifici Prefabbricati."*

Magliulo, G., Cimmino, M., Ercolino, M., & Manfredi, G. (2014). Prove cicliche a taglio sulla connessione SicurlinkTM tra trave e pilastro prefabbricati (in Italian). *Proceedings of Workshop "Tecniche Innovative per Il Miglioramento Sismico Di Edifici Prefabbricati."*

Magliulo, G., Ercolino, M., Petrone, C., Coppola, O., & Manfredi, G. (2014). The Emilia Earthquake: Seismic Performance of Precast Reinforced Concrete Buildings. *Earthquake Spectra*, *30*(2), 891–912. https://doi.org/10.1193/091012EQS285M

Martinelli, P., & Mulas, M. G. (2010). An innovative passive control technique for industrial precast frames. *Engineering Structures*, *32*(4), 1123–1132. https://doi.org/10.1016/j.engstruct.2009.12.038

Mashal, M., Palermo, A., & Keats, G. (2019). Innovative metallic dissipaters for earthquake protection of structural and non-structural components. *Soil Dynamics and Earthquake Engineering*, *116*, 31–42. https://doi.org/10.1016/J.SOILDYN.2018.10.002

Muciaccia, G., Cervio, M., Franzoso, M., & Veneziano, M. (2014). Utilizzo di ancoraggi post-inseriti in interventi di recupero di capannoni industriali in zona sismica (in Italian). *Proceedings of Workshop "Tecniche Innovative per Il Miglioramento Sismico Di Edifici Prefabbricati."*

Palermo, A., Pampanin, S., & Calvi, G. M. (2005). CONCEPT AND DEVELOPMENT OF HYBRID SOLUTIONS FOR SEISMIC RESISTANT BRIDGE SYSTEMS. *Journal of Earthquake Engineering*, *9*(6), 899–921. https://doi.org/10.1080/13632460509350571

Pampanin, S., Marriott, D., & Palermo, A. (2010). *PRESSS design handbook*. NZCS.

Pollini, A.V., Buratti, N., & Mazzotti, C. (2020). Behaviour factor of concrete portal frames with dissipative devices based on carbon-wrapped steel tubes. *Bulletin of Earthquake Engineering*. https://doi.org/10.1007/s10518-020-00977-y

Pollini, A.V., Buratti, N., & Mazzotti, C. (2018). Experimental and numerical behaviour of dissipative devices based on carbon-wrapped steel tubes for the retrofitting of existing precast RC structures. *Earthquake Engineering & Structural Dynamics*, *47*(5), 1270–1290. https://doi.org/10.1002/eqe.3017

Priestley, M. J. N., Sritharan, S. S., Conley, J. R., & Pampanin, S. (1999). Preliminary results and conclusions from the PRESSS five-story precast concrete test building. *PCI Journal*, *44*(6), 42–67. https://doi.org/10.15554/PCIJ.11011999.42.67

Savoia, M., Buratti, N., & Vincenzi, L. (2017). Damage and collapses in industrial precast buildings after the 2012 Emilia earthquake. *Engineering Structures*, *137*, 162–180. https://doi.org/10.1016/j.engstruct.2017.01.059

Schultz, A. E., & Magana, R. A. (1994). SEISMIC BEHAVIOUR OF CONNECTIONS IN PRECAST CONCRETE WALLS. *Mete A. Sozen Symposium. A Tribute from His Students*, 273–311.

Twigden, K. M., & Henry, R. S. (2015). Experimental response and design of O-connectors for rocking wall systems. *Structures*, *3*, 261–271. https://doi.org/10.1016/J.ISTRUC.2015.06.002